

Recent Progresses in Atmospheric Remote Sensing Research in China ——Chinese National Report on Atmospheric Remote Sensing Research in China during 1999–2003

QIU Jinhuan* (邱金桓), and CHEN Hongbin (陈洪滨)

Institute of Atmospheric Physics, Chinese Academy of Sciences, Beijing 100029

(Received 6 March 2003; revised 15 September 2003)

ABSTRACT

Progresses of atmospheric remote sensing research in China during 1999–2003 are summarily introduced. This research includes: (1) microwave remote sensing of the atmosphere; (2) Lidar remote sensing; (3) remote sensing of aerosol optical properties; and (4) other research related to atmospheric remote sensing, including GPS remote sensing of precipitable water vapor and radiation model development.

Key words: remote sensing, microwave, Lidar, aerosol optical property

1. Microwave remote sensing of the atmosphere

1.1 *Ground-based*

1.1.1 *Active microwave remote sensing*

In recent years, great progress has been made in the development of weather radar hardware. According to the specifications of new generation weather radar systems stimulated by the China Meteorological Administration (CMA), a Doppler weather radar operating in the C-band, named CINRAD/CC, has been successfully designed by Anhui Sun-Create Electronics Co., Ltd. The radar is a blend of the latest radar and computer technology with valuable experience accumulated by weather analysis experts and radar observers. It can not only measure the reflectivity factor but also the wind field in precipitating clouds. In the same manufacturing unit are fabricated the C-band conventional and digital radar (JY-16A series) and X-band radar (JY-28 series) mainly for rainfall measurements.

In order to enhance the capability of observing precipitating clouds, a dual-wavelength (X/Ka) and dual-polarization radar has been developed and combined into an active and passive microwave system in the Institute of Atmospheric Physics of the Chinese Academy of Sciences (IAP/CAS). This undated system has played an important role in monitoring and tracking the heavy storm over Beijing in the summer

of 2001 (Duan et al., 2002).

For obtaining 3-D wind profiles up to the lower stratosphere, a Doppler wind profiler radar has been developed by the Institute No.23 of the China Aerospace Science and Industry Corporation. The radar system CFL-20, a fully coherent phased array pulsed Doppler radar, is composed of two radars operating at 918 MHz (UHF) and 48 MHz (VHF), respectively. The UHF radar measures the boundary wind profile while the VHF radar monitors the wind distribution from 2.5 to 25 km. The system can provide the wind profiles in real time in all weather conditions with automatic data processing and display, intelligent monitoring system, and several operation modes. A radio-acoustic sounding system (RASS) can also be included in the system for temperature measurements in the boundary layer.

A powerful VHF/ST radar, designed by the IAP, operates from time to time at the Xianghe Observation Station of IAP for collecting data of wind and its variance profiles between 2–20 km for use in the stratosphere-troposphere exchange study. The wuhan Institute of Physics and Mathematics (WIPM) of the CAS has also established an MF (Middle Frequency) Doppler radar for mesospheric wind measurement. A Rayleigh and Sodium Lidar system at WIPM operates quasi-continuously for observing the sodium layer and middle atmospheric density profiles (Lu et al., 2002).

*E-mail: jhqui@mail.iap.ac.cn

As a milestone in the development history of the weather radar network in China, the American NEXRAD (Next Generation Radar) (WSR-88D) was introduced in 1998 and then the CINRAD radar was successfully fabricated by a joint company (MET-STAR). The CINRAD's radar, almost the most advanced weather radar in use, is so sensitive that it can detect and display clear air returns with unparalleled detail even in the less sensitive volume coverage patterns. It provides many products to weather forecasting experts and other users, such as storm total precipitation, wind velocity and direction, VAD (velocity-azimuth display) wind profile, wind shear, tornado detection, microburst detection, and so on. The establishment of a CINRAD network covering continental China is under way.

In parallel, during last four years there have been many research works on the applications of ground-based radar data in weather forecasting, data assimilation experiments, numerical modeling, and so on. The detailed description of these works is out of the scope of this review paper.

1.1.2 *Passive microwave remote sensing*

Along with the advance of microwave radiometric technology in China, passive microwave remote sensing has been applied widely in determining atmospheric precipitable water (PW), liquid water path (LWP), rainfall, and even the temperature profile.

Lei et al. (2001) applied a dual-wavelength microwave radiometer to detect PW and LWP before precipitation passages in Xi'an City from August to November in 1997. The observation results show that there is a sharp increase both in PW and LWP before all precipitation. It is indicated that in the precipitation region there is an accumulation or convergence of PW and cloud liquid water from the plentiful area around. It is suggested that these observed phenomena should be considered in weather now-casting and modifications.

The difficulties encountered in microwave radiometric observations in the rainy atmosphere were investigated by Wei et al. (2001). They introduced a scheme to correct the effect of liquid water on the antenna system and a method for retrieving PW and LWP and presented a statistical analysis of microwave radiometer measurements in rainy atmospheres. The results indicate that when the rain rate R is less than 20 mm h^{-1} , there always exists the possibility to obtain PW and LWP measurements with relative errors less than 5% and 20% respectively. In the statistical sense, some parameters like precipitation effectiveness and potentiality were obtained from the ground-based

microwave radiometer observations.

1.2 *Space-based*

1.2.1 *Active remote sensing*

Dou and Testud (1999) did a study on the application of stereo-radar analysis to space-borne rain radar. Due to the current technical constraints, the space-base precipitation radar has to work at the rain attenuated wavelength to satisfy the requirements of high spatial resolution, wide coverage, large dynamic range of rainfall measurements, and accurate point precipitation measurements. The stereo-radar analysis is used as a procedure to correct the attenuated reflectivity field by using the apparent reflectivity observed by radars along the radar's two viewing angles and to retrieve the specific attenuation coefficient field. They studied the influence of the non-uniform beam filling effect due to the implementation of space-borne means on the stereo-radar analysis.

The precipitation characteristics over the Tibetan Plateau were synthetically investigated by Fu et al. (2002) using TRMM (Tropical Rainfall Measurement Mission) products of 2A25 from the Precipitation Radar (PR) and 1B11 from the TRMM Microwave Imager (TMI). Their investigation shows that stratiform precipitation in the Tibet region is a dominant type according to the NASA/GFSC (Goddard Flight Space Center) PR algorithm. Statistics show that area fraction ratio of stratiform to convective rains is at least 20. Even in summer, the ratio reaches 10. As a result, stratiform rains form much more rainfall than convective rains, the former being at least 2 times larger than the latter. In their investigation, the vertical profiles of precipitation and corresponding TMI brightness temperatures (TBs) were also compared between these two types of rain.

A method was proposed by Chen (2002) to determine LWP from microwave attenuation by clouds along the satellite-earth surface path. He conducted an investigation on the optimal choice of channels, observation modes, and error analyses. The results show that (a) in principle, the proposed method can provide LWP measurements with much better accuracy than available (passive) satellite remote sensing; (b) the method using a dual- or triple-channel combination can simultaneously measure precipitable water, LWP, and ice water path (IWP); and (c) if combined with the available satellite remote sensing techniques, it would more efficiently yield global datasets of LWP, PW, and IWP.

1.2.2 *Passive remote sensing*

By using a physical-statistical method, Chen (2000) developed a retrieval algorithm for determin-

ing cloud LWP over oceans from SSMI (Special Sensor Microwave Imager) measurements. A simple relation was obtained between the LWP and the difference of TBs in cloudy and clear atmospheres ΔTB from the simulation dataset yielded by means of a radiative transfer model. In his algorithm, only the relationship LWP- ΔTB in the channel of vertically polarized 37 GHz (37V) is used because it has smaller rms errors. The TB at 37V in 'clear' atmosphere can be derived through a relationship with TB at 19V obtained by regression of SSMI observation data in really clear atmospheres. Comparison of LWP results retrieved from the SSMI measurements by the proposed algorithm and the other two algorithms of Alishouse et al. (1990) and Weng et al. (1997) shows that Chen's retrieval algorithm yields quite reliable retrievals of cloud liquid water path over oceans.

Liu et al. (2001) also developed a cloud LWP retrieval algorithm optimized for the tropical atmospheric conditions for the Airborne Imaging Microwave Radiometer (AIMR) measurements during the 1999 observation period of the INDOEX (Indian Ocean Experiment). Radiative transfer modeling and error analyses were conducted to guide the selection of AIMR channels used for the LWP retrievals. Results show that the horizontal polarization channels outperform the vertical polarization channels at both 37 and 90 GHz. Additionally, for LWP less than 300 g m^{-2} , the best results are expected from the 90 GHz horizontal polarization channel, while the 37 GHz horizontal polarization channel performs better for higher LWP values. On the basis of these findings, they formulated the LWP retrieval algorithm from the combination of retrievals of the 37 and 90 GHz horizontal polarization channels. Results of several indirect validations show that in nearly clear conditions the LWP retrievals have an rms error of about 28 g m^{-2} but with a near zero mean bias.

The combined data from a ground-based dual wavelength (1.35 and 0.8 cm) microwave radiometer and the TRMM/TMI were used to retrieve the cloud liquid water amount over the Shouxian area of Anhui by Yao et al. (2001). Based on statistical regression, the retrieval algorithm for LWP was derived using only the brightness temperature data in the 85 GHz-V channel. Analysis results show that (a) there exists a threshold of 0.4 mm cloud LWP in the area, and (b) when the LWP is larger than this threshold, precipitation will occur. There appears a noticeable increase (decrease) in PW and LWP before (after) the

precipitation.

2. Lidar remote sensing of the atmosphere

This section introduces the main developments in the Lidar technique and its application in China during 1999–2003.

2.1 Lidar measurements of ozone, cloud, and aerosols

A four-wavelength Lidar system has been recently developed at the IAP/CAS for monitoring the 10–40 km ozone profile, the 2–40 km aerosol profile, and high cloud optical properties (Qiu et al., 2002a; 2003a). It contains a XeCl excimer laser with output energy of about 120 mJ at 308 nm, a Nd-YAG (Yttrium Aluminium Garnet) laser with three operating wavelengths of 355 nm, 532 nm, and 1064 nm, and a 1 m-receiving telescope. There are four analog-detection channels and two photon-counting channels. Three among four analog channels are used for detections of the 532 nm backscattering (two for polarization detection), and another for the 355 nm radiation. Two photon-counting channels of 308 nm and 355 nm are for ozone measurements. Two examples of ozone and aerosol measurement results by the Lidar are shown in Figs. 1–2.

Figure 1 shows a comparison of the ozone concentration profile measured by the Lidar on 16 October 2001 via a balloon-borne Electronic-Chemistry Cell (ECC) in Beijing. A good agreement between both profiles is obtained, especially in the height range from 10 km to 20 km. As shown in Fig. 2, there is an aerosol layer ranging from about 4 km to 10 km, where the

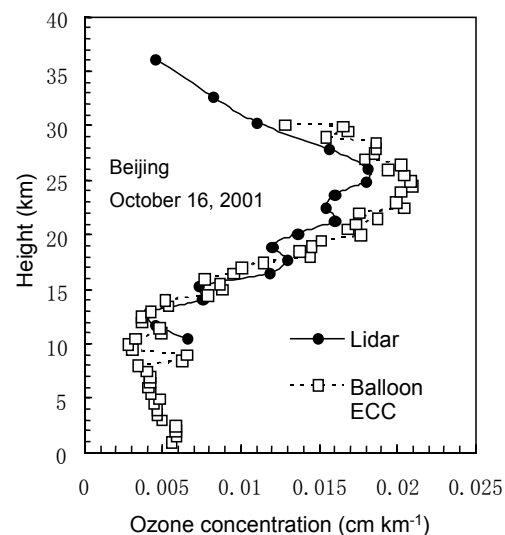


Fig. 1. A comparison between ozone concentration profiles by Lidar and balloon (ECC).

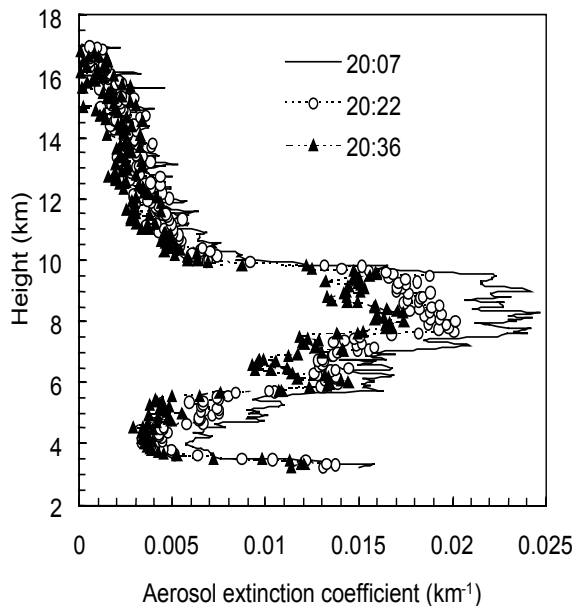


Fig. 2. Aerosol extinction coefficient profiles measured by the four-wavelength Lidar during a dust-storm event in the Beijing area on 7 April 2000.

Lidar-measured aerosol extinction coefficient profiles during 2007–2036 LST 7 April 2000 look like a typical normal distribution with the coefficient maximum value at about 8 km. On 6 April 2000, a very strong dust-storm passed over the Beijing area, and on 7 April no cloud was observed. So, the aerosol layer may be a mineral particle layer, transported from remote desert areas.

In addition, Hu's group at the Anhui Institute of Optics and Fine Mechanics (AIOFM) used a NASA-made Multiple Pulse Lidar (MPL) to detect aerosol extinction coefficient profiles in the troposphere over Beijing areas (Hu et al., 2002). Bai et al. (2000) used a Japan-made Lidar to measure the optical properties of stratospheric and tropospheric aerosols over Lhasa areas.

2.2 Lidar measurements of temperature, moisture, and wind profiles

Lidar is a potential means for remote sensing of four basic meteorological parameters, namely temperature, moisture, pressure, and wind in the clear atmosphere.

Li et al. (2000) developed a Raman Lidar system for monitoring the water vapor profile. By using the Lidar, the water vapor mixing ratio is measured over the city of Hefei. In their study, the characteristics and the errors of typical water vapor mixing ratio profiles detected by the Lidar are analyzed.

Two kinds of lidars for wind measurements have been developed in China. One is incoherent Doppler

wind Lidar, developed by Liu et al. (1997) at Qingdao Ocean University for measurements of the tropospheric wind. The Lidar uses an iodine vapor filter to separate the Mie and Rayleigh scattering components, and it discriminates the Doppler shift frequency by using a double edge technique. Based on the Doppler Lidar, now Liu's group is developing a high spectral resolution Lidar (HSRL) system for simultaneous measurements of wind and aerosol optical properties. As shown in simulations presented by Liu et al. (2003), the error of wind velocity below an altitude of 20 km is smaller than 2 m s^{-1} , and the error of the aerosol backscattering coefficients is smaller than 30% if HSRL is employed in the night. In the daytime, the Lidar system can remotely sense wind velocity and aerosol backscattering coefficients within an altitude of 10 km with the same accuracy. Another kind of wind Lidar, developed at the IAP/CAS, uses a correlation-analysis technique (Yang, 1999), in which the inhomogeneous aerosol is treated as a wind tracer.

Measurements of thermal profiles in the stratosphere and mesosphere with Rayleigh scattering Lidar were made at the AIOFM, presented by Wu et al. (2002), and at the Wuhan Institute of Physics & Mathematics (WIPM), Chinese Academy of Sciences (Zheng et al., 1999). As shown in Wu et al. (2002), thermal profiles obtained by the Rayleigh Lidar agree very well with satellite UARS/HALOE (Upper Atmosphere Research Satellite/Halogen Occultation Experiment) and radiosonde observations. In the study by Zheng et al. (1999), the atmospheric density profile ranging from 30 to 70 km and the temperature profile from 30 to 60 km over Wuhan were measured by the Rayleigh scattering Lidar.

2.3 Lidar measurements of trace pollution gases

A new mobile Lidar to monitor atmospheric pollution in the troposphere was recently developed by the Zhang group at AIOFM (Zhang et al., 2001, 2002). The Lidar can measure SO_2 , NO_2 , O_3 , and aerosol profiles with the maximum ranges of 3 km, 4 km, 3 km, and 5 km, and the minimum monitoring concentrations of 4, 20, 4, and 0.05 ppb km^{-1} , respectively.

3. Remote sensing of aerosol optical properties

Atmospheric aerosols are receiving more and more concern because of their significant climate forcing and the atmospheric correction of space-borne remote sensing (Mao et al., 2002; Menon, 2002; Charlson et al., 1992; Penner et al., 1994). It is found that sulfate aerosol, carbonaceous aerosol, and mineral dust have

a substantial climatic forcing in clear sky which is comparable with the effect of greenhouse gases. But the estimates are still uncertain in quantity. Among all the reasons, the lack of information of aerosol optical properties, especially its absorption, is a significant one (Penner et al., 1994). In order to enrich aerosol information, many Chinese investigators have made great efforts to develop remote sensing methods of aerosol optical properties and to use them in determining the properties of aerosols in China. These developments are introduced as follows.

3.1 *Satellite remote sensing of aerosol optical properties*

There has been a long history of ground-based observations of atmospheric aerosol optical properties by sunphotometer. Ground-based measurements, however, cannot provide aerosol parameters over large areas. Satellite remote sensing is the sole means to determine aerosol properties on the global scale. In fact, in the last 30 years, research on satellite remote sensing of aerosols has made important progresses. At present, there are two main methods for the remote sensing of aerosols. The first one is the occultation method in which the stratospheric aerosol extinction coefficient profile is determined by measuring the attenuated solar direct radiation at sunrise and sunset with a radiometer. This method has a shortcoming in determining the tropospheric aerosol optical properties. Another is to retrieve the atmospheric column aerosol optical depth from outgoing sky radiance measured in space, which is mainly applied under the situation of an ocean underlying surface. There is generally a stronger and more complex effect of the land surface on upward sky radiance. Therefore, satellite remote sensing of aerosols over land leaves some questions, especially in the case of a high-reflectance surface. It is very important to develop new and reliable methods of satellite remote sensing of aerosols over land. In recent years, many new methods have been developed by Chinese researchers. These developments include:

(1) Based on the vegetation reflectance properties from near ultra-violet to near infrared and the extraterrestrial radiance sensitivity to vegetation reflectance and atmospheric Aerosol Optical Depth (AOD), Qiu (1999a) proposed a method for satellite synthetic remote sensing of the surface reflectance and AOD by using a corresponding iteration-correlation inversion algorithm. According to numerical simulations, effects of radiance error, aerosol imaginary index uncertainty, and vegetation medium inhomogeneity on the retrieved result are analyzed. Inversion results show that the effect of the imaginary index uncertainty

is very important. As the error of the aerosol imaginary index is within 0.01, standard errors of aerosol optical depth and vegetation reflectance solutions using 14 spectral channels from 410 nm to 900 nm are respectively less than 0.063 and 0.023.

(2) Based on an analysis of sky radiance distribution on aerosol optical properties and surface albedo, Zhao and Mao (1999) developed a method for simultaneous retrievals of AOD, aerosol single scattering albedo, and surface albedo from the radiance and visible channel data of GMS5.

(3) By simulating the sensitivity of GMS5 apparent reflectance to the surface reflectance and AOD, Mao et al. (2001) developed a method to determine AOD over lakes from GMS5 data. Some comparisons of the GMS5 measurements with sunphotometer measurements showed that the relative error of monthly mean AOD at 533.6 nm is less than 30%. The method is further developed to measure AODs over 25 lakes in China (Zhang et al., 2003). This method is based on the lower lake reflectance. If the lake reflectance is greatly different than the surrounding land surface reflectance, there may be a significant adjacency effect on the GMS5 apparent reflectance from the lake, which can result in a larger error in the AOD retrieval.

(4) Based on the weak dependence of the upwelling solar radiance from a cloud-shadow surface upon the surface reflectance, Duan (2001) proposed a new dark-subject method to retrieve AOD from satellite data (using the cloud-shadow surface as a dark-subject). This method is confronted with a difficulty to determine the inhomogeneous radiance field in the broken cloud case.

(5) Han (2000) proposed a method to retrieve optical properties of aerosols over grassland from satellite data of outgoing scalar and polarized radiances.

3.2 *Broadband solar radiation methods for aerosol retrievals*

In recent years, some researchers have paid great attention to develop the broadband extinction methods to retrieve AOD from pyrhemeter data and their applications (Gueymard, 1998; Molineaus et al., 1998; Luo et al., 2001; Qiu, 1998, 2001a; Qiu and Yang, 2000; Zhou et al., 1998), being impelled mainly by two reasons. At first, AOD is an important and convenient parameter for studies of atmospheric pollution, aerosol radiation-climate effect, and so on. Secondly, there is a worldwide pyrhemeter network for broadband direct solar radiation observations, and high-quality historic broadband radiation data go back to the 1880s (Stothers, 1996). Therefore, the quantitative method to retrieve AOD from pyrhemeter data is very useful.

A method to determine the 0.75 μm AOD from pyrliometer data is proposed by Qiu (1998). Considering the effect of uncertainty in the aerosol size distribution on the AOD retrieval (Qiu, 1998), Qiu (2001a) developed a new broadband extinction method to retrieve the AOD. In the method, a parameterized expression of the ‘equivalent’ wavelength, at which AOD is equal to Broadband AOD (BAOD), is developed, and then the λ -wavelength AOD is determined in terms of the ‘equivalent’ wavelength and the BAOD. In addition, an approach to determine both the Ångström wavelength index and the AOD from pyrliometer data with large solar zenith angles is proposed. In these methods the solar zenith angle cosine (μ_0) is needed. Pyrliometer data are usually recorded in the format of hourly/daily/monthly accumulated radiation. During the accumulated period the solar zenith angle is variable, and hence a problem is how to select a suitable μ_0 for the AOD retrieval. Due to highly variable and random cloud cover distribution, there may often be cloud effects on the accumulated direct solar radiation, especially in the two cases of daily and monthly pyrliometer data. For these reasons, some available approaches to use hourly/daily/monthly accumulated radiation data for the AOD retrievals are developed (Qiu and Yang, 2002b; Qiu, 2003b).

On the other hand, based on the diffuse-direct method to retrieve the aerosol imaginary part developed by Herman et al. (1975), Wei and Qiu (1998, 2000) developed a broadband diffuse method for the imaginary part retrieval from paranometer data. The paranometer used in China has a shading ring to shade direct solar radiation to yield the diffuse radiation, and the shaded light scattering effect is corrected. Considering the uncertainty in the correction, Qiu and Yang (2002c) improved the broadband diffuse radiation method. The first improvement is to determine diffuse radiation from combined pyrliometer and paranometer data in order to avoid the shading ring correction. Secondly, some available approaches to input relative parameters are presented.

3.3 *Optical properties of aerosols in China*

In recent years, research on optical properties of aerosols over China mainly focus on the following three aspects: (1) long-term variation characteristics and distinct-distribution properties of AODs in China; (2) aerosol imaginary part and its single scattering albedo characteristics; (3) aerosol extinction coefficient profiles over some areas, especially first one.

3.3.1 *Aerosol optical depth characteristics*

By using the broadband extinction method, Qiu and Yang (2000) studied the variation characteristics

of atmospheric optical depths in North China during 1980–1994. As shown in the study, during 1980–1994 the AODs show an increased trend, and in the winter the trend is stronger, and there is an evident Pinatubo effect on the AODs in China.

By using a method improved from Qiu’s broadband extinction method, Luo et al. (2001, 2002) retrieved and analyzed AODs over 46 meteorological stations in China for the period 1961–1990. It was found that the yearly mean AOD has a pattern related to the geographical features with the maximums over basins. One of the maximum centers is at Sichuan Basin in Southwest China, and the other is in the south Xinjiang Basin in Northwest China. In most areas of China the maximum AOD occurs in spring. In addition, AOD increased dramatically over mainland China from 1961 to 1990, particularly in the middle and lower reaches of the Yangtze River and the east part of Southwest China. In North China, Shandong Peninsula, the east part of the Qinghai Province, and the coastal areas of the Guangdong Province, a significant increasing trend of AOD is shown, while in most parts of Northwest and Northeast China, the increase trend is less significant. For the total of the 46 stations, the yearly averaged AOD variation curve can be briefly divided into two periods. One period is from 1961 to 1975, when the AOD is smaller than the 30-year mean value; the other period is from 1976 to 1990, when the AOD is higher than the mean value.

Some research on the GMS5 remote sensing of aerosol optical depths over 25 lakes in China are contributed by Mao’s Group (Mao et al., 2002; Zhang et al., 2003). Based on TOMS/AI and aerosol optical depth data provided by the NASA/TOMS aerosol group, Xia (2002) analyzed the temporal and spatial distribution characteristics of aerosols, especially dust aerosols in North China. The trend analysis of dust aerosol concentration shows a distinct spatial distribution in North China, from west to east, with a declining magnitude that decreases slowly.

In addition, Zhang et al. (2002a, b) used some multi-wavelength sunphotometers to measure AODs over Beijing and the Damxung region, Tibetan Plateau.

3.3.2 *Aerosol imaginary part and its single scatter albedo characteristics*

By using the broadband radiation method, Wei and Qiu (2000) retrieved the aerosol imaginary part (AIP) in Beijing during 1992 from paranometer data. The retrieval results show that the monthly mean AIPs in January, February, and December are 0.053, 0.064, and 0.050, respectively, being larger than those in

other months. Later, by using an improved broadband radiation method, Qiu and Yang (2002b) retrieved and analyzed AIP and aerosol single scattering albedo in Beijing and Shenyang during 1993–2000 from joint pyrhelimeter and paranometer data. It is shown that the Beijing yearly mean AIP and aerosol scattering albedo change from 0.021 to 0.026 and from 0.816 to 0.85 during 1993–2000, and the total mean AIP and albedo are 0.0234 and 0.833, respectively. In Shenyang, the AIPs during 1993–1996 are evidently larger than those during 1997–2000, and the total mean AIP and albedo are 0.0336 and 0.782, respectively. There is the (larger AIP) stronger absorption of aerosols in Shenyang.

3.3.3 Aerosol extinction coefficient profiles

Hu's group used a NASA-made Multiple Pulse Lidar (MPL) to detect aerosol extinction coefficient profiles in the troposphere over Beijing areas (Hu et al., 2002), and Bai et al. (2000) used a Japan-made Lidar to measure the optical properties of stratospheric and tropospheric aerosols over Lhasa areas.

4. Other remote sensing research

Apart from the above three aspects, during 1999–2003 Chinese scientists also made some significant progresses in the remote sensing research of precipitable water (using the GPS technique), ozone, lightning, radiation, and so on.

4.1 GPS remote sensing of precipitable water vapor

Recently some Chinese researchers have placed their efforts into GPS remote sensing of precipitable water vapor. By using the regional ground-based GPS network in Beijing, Liang et al. (2003) estimated the atmospheric water vapor from the data of the GPS/VAPOR experiment with high time resolution. In this study, the relation between the ground vapor pressure and precipitation is analyzed. The precipitable water from GPS data is well related with the ground water vapor pressure on a clear day, but not well on cloudy or rainy days. An abrupt increase of regional atmospheric water vapor in a short time is often accompanied by precipitation, although the value of the integrated precipitable water does not correspond to the amount of precipitation. Wang et al. (1999) collected six-day GPS data provided by 23 national stations for ground experiments. After separating the dry and wet zenith delay and transforming the wet zenith delay into precipitable water vapor, the precipitation is derived with a precision up to 1–2 mm. There is a good coincidence of the results based on

GPS with those based on radiosonde data. Li et al. (1999) used GPS data over the Shanghai and Wuhan areas during summer in 1997 for precipitable water retrievals with a half-hour resolution. The standard deviation of the precipitations from GPS data with those from radiosonde data is about 0.5 cm. In addition, Li and Mao (1999) developed an approach to the remote sensing of water vapor based on GPS and linear mean temperature in the eastern region of China.

4.2 Remote sensing of ozone, lightning, and UVB irradiance

Xia and Wang (2001) developed a new method for inferring total ozone and aerosol optical thickness from multispectral extinction measurements using eigenvalue analysis. By using about 20 years of Dobson and TOMS data, Bian et al. (2002) analyzed the variation characteristics of total atmospheric ozone in Beijing and Kunming. It is shown that the long-term change trends for the 1979 (or 1980)–2000 period are $-0.642 \text{ DU yr}^{-1}$ and $-0.009 \text{ DU yr}^{-1}$ respectively in Beijing and Kunming. In addition, there are significant QBO signals both in Beijing (mid latitude) and Kunming (low latitude).

Observations of lightning from space have been made for more than 30 years. Chen and Lu (2001) presented the satellite-borne instruments for lightning detection and mapping with focus on the lightning optical sensors. They also summarized some important results obtained from the observation data analysis.

Wang et al. (2001) developed a new parameterization method for retrieving surface UVB irradiance and erythral UVB (Ultra Violet B) radiative dose rate. This method is based on a simple concept: the earth-atmosphere system can be equivalent to three layers: the absorption layer by ozone, the scattering layer containing air molecules, cloud and aerosol particles, and the surface reflection. The surface UVB irradiance and erythral UVB dose rate can be expressed by the effective transmission of the ozone layer and united reflectivity due to the scattering layer and the surface. An actual application has been performed using satellite observations, and the results are compared with the surface observations, showing a good agreement.

4.3 Radiation models for remote sensing applications

Some radiation models have been developed for remote sensing applications.

The fractional factor f of δ -function scaling in the δ -Eddington approximation modifies the fractional scattering into the forward peak. As shown in the paper presented by Qiu (1999b), a reasonable choice of

the fractional factor f of δ -function scaling in the δ -Eddington approximation can yield a great improvement of the transmission, reflection, and absorption calculations in the condition of the optical depth $\tau_t \leq 1$. Based on the fact, a modified δ -Eddington approximation is empirically and mathematically developed using a parameterization model of the factor f , which mainly depends on the asymmetry factor g_0 , total optical depth τ_t , single scattering albedo, $\bar{\omega}$ (ground) surface reflectance A , and cosine of solar zenith angle μ_0 . In an average sense, in the condition of $A \leq 0.6$, $\tau_t \leq 1$, $0.1 \leq \mu_0 \leq 1.0$, and $0.5 \leq \omega \leq 1$, the modified δ -Eddington approximation can reduce transmission, reflection, and absorption errors by a factor of about two, compared with the results by the δ -Eddington approximation.

Based on the 6S mode (Vermeete et al., 1997), an improved model of the surface BRDF (Bidirectional Reflectance Distribution Function)-atmospheric coupled radiation is proposed by Qiu (2001b), in which the key point is an upward flux correction. As shown in comparative numerical simulations, this model generally has a better accuracy than some existing models. In the condition of the solar zenith angle $\theta_s \leq 75^\circ$ and the viewing angle $\theta_v \leq 60^\circ$, the error by Qiu's model is usually smaller than 2.5%.

In addition, a parameterized atmospheric correction model and a simple yet more accurate code to calculate solar radiative flux in the optically inhomogeneous atmosphere are developed by Qiu (2001c; 2002c). By using least squares technology, in the atmospheric correction model the path radiance is parameterized in terms of atmospheric optical depth, single scattering albedo, solar zenith angle, viewing zenith angle, azimuth angle, and atmospheric asymmetry factor. As shown in the numerical simulations, for the four MODIS channels of 865 nm, 670 nm, 550 nm, and 412 nm, the solar zenith angle from 0° to 70° , the viewing zenith angle of 0° to 66° , and the surface reflectance of 0.05 to 0.8, standard errors of the parameterized upwelling radiance are less than 4%.

REFERENCES

- Alishouse, J. C., S. Snider, E. R. Westwater, C. Swift, C. Ruf, S. Snyder, J. Vongsathorn, and R. R. Ferraro, 1990: Determination of cloud liquid water content using the SSMI. *IEEE Trans. Geosci. Remote Sens.*, **28**, 817–822.
- Bai Yubo, Shi Guangyun, K. Tamura, and Y. Iwasaka, 2000: Lidar observations of atmospheric aerosol optical properties over Lhasa. *Chinese J. Atmos. Sci.*, **24**, 559–567.
- Bian Yangliang, Chen Hongbin, Zhao Yangliang, and Lu Daren, 2002: Variation features of total atmospheric ozone in Beijing and Kunming based on Dobson and TOMS data. *Adv. Atmos. Sci.*, **19**, 279–286.
- Charlson, R. J., S. E. Schwartz, J. M. Hales, R. D. Cess, J. A. Coakley, Jr., J. E. Hansen, and D. J. Hofmann, 1992: Climate forcing by anthropogenic aerosols. *Science*, **255**, 423–429.
- Chen Hongbin, and Lu Daren, 2001: Observations of lightning from space: A review. *Acta Meteorologica Sinica*, **59**, 377–383.
- Chen Hongbin, and Lu Daren, 2000: A retrieval algorithm for deriving liquid water path from space-borne microwave radiometric measurements. *Journal of Remote Sensing*, **4**(3), 165–171. (in Chinese)
- Chen Hongbin, and Lu Daren, 2002: A concept for measuring liquid water path from microwave attenuation along the satellite-Earth path. *Chinese J. Atmos. Sci.*, **26**(4), 402–408. (in Chinese)
- Dou, X. K., and J. Testud, 1999: The application of stereoradar analysis to the spaceborne rain radar. *Acta Meteorologica Sinica*, **57**(3), 358–366. (in Chinese)
- Duan Mingzheng, 2001: Simultaneous retrieval of atmospheric aerosol optical thickness and surface albedo over land by using polarized radiance as well as solar radiance from satellite measurement. Ph. D. dissertation, Institute of Atmospheric Physics, 108pp. (in Chinese)
- Duan Shu, Zhang Ling, Liu Jinli, and Lu Daren, 2002: Development of an active and passive dual-wavelength (X/Ka) and dual-polarization remote sensing system and its preliminary test. *Journal of Remote Sensing*, **6**, 289–293. (in Chinese)
- Fu, Y., G. Liu, and Y. Lin, 2002: Rainfall in Tibetan Plateau as viewed by TRMM satellite. *TRMM International Science Conference*, Hawaii.
- Gueymard, C., 1998: Turbidity determination from broadband irradiance measurements: A detailed multicoefficient approach. *J. Appl. Meteor.*, **37**, 414–435.
- Han Zhigang, 2000: Satellite remote sensing of aerosol optical properties over grass by using polarized radiance. Ph. D. dissertation, Institute of Atmospheric Physics, 104pp. (in Chinese)
- Herman, B. M., S. R. Browning, and J. J. De Luisi, 1975: Determination of the effective imaginary term of the complex refractive index of atmospheric dust by remote sensing: The diffuse-direct radiation method. *J. Atmos. Sci.*, **32**, 918–925.
- Hu Huanling, Xie Chenbo, Yan Fengqi, Qiu Xiangshuang, and Yu Tong, 2002: Lidar measurements of aerosol-layer near the ground with actual extinction-backscatter-ratio in BAPIE. *Proc. 21th ILRC*, Quebec, Canada, 161–164.
- Lei, H. C., C. Wei, Z. L. Sun, L. Gu, and L. Yan, 2001: Microwave radiometric measurement of water vapor and cloud liquid water before rainfall. *Quarterly Journal of Applied Meteorology*, **12** (Suppl.), 73–78. (in Chinese)
- Li Chengcai, Mao Jietai, and Li Jiangguo, 1999: GPS remote sensing of total water vapor amount. *Chinese Science Bulletin*, **3**, 333–336.
- Li Jiangguo, and Mao Jietai, 1999: The approach to remote sensing of water vapor based on GPS and linear Tm in eastern region of China. *Acta Meteorologica Sinica*, **12**, 450–458.

- Li Tao, Qi Fudi, Jin Chuanjia, Yue Guming, Hu Huanling, and Zhou Jun, 2000: Raman Lidar system for the measurements of water vapor mixing ratio in the atmosphere. *Chinese J. Atmos. Sci.*, **24**, 843–854.
- Liang Feng, Li Chengcai, Wang Yingchun, Mao Jietao, and Fang Zongyi, 2003: An analysis of atmospheric precipitable water based on regional ground-based GPS network in Beijing. *Chinese J. Atmos. Sci.*, **27**, 236–244.
- Liu Guosheng, J. A. Curry, J. A. Hargerty, and Fu Yunfei, 2001: Retrieval and characterization of cloud liquid water path using airborne passive microwave data during INDOEX. *J. Geophys. Res.*, **106**, 28719–28730.
- Liu Jintao, Chen Weibiao, and Liu Zhishen, 2003: A simulation of simultaneously measuring wind and aerosol optical properties using high spectral resolution Lidar. *Chinese J. Atmos. Sci.*, **27**, 115–122.
- Liu Zhishen, Chen Weibiao, T. L. Zhang, J. W. Hair, and C. Y. She, 1997: An incoherent Doppler Lidar for ground-based atmospheric wind profiling. *Appl. Phys. (B)*, **64**, 561–566.
- Lu, D. R., F. Yi, and J. Y. Xu, 2002: Advances on study of middle and upper atmosphere and their coupling with lower atmosphere. *Chinese J. Space Sci.*, **22**(Suppl.), 111–119.
- Luo Yunfeng, Lu Daren, Zhou Xieji, Li Weilian, and He Qing, 2001: Characteristics of the spatial distribution and yearly variation of aerosol optical depth over China in last 30 years. *J. Geophys. Res.*, **106**(D13), 14501–14513.
- Luo Yunfeng, Lu Daren, Zhou Xieji, Li Weilian, and He Qing, 2002: Analyses on the spatial distribution of aerosol optical depth over China in recent 30 years. *Chinese J. Atmos. Sci.*, **26**, 721–730.
- Mao Jietai, Liu Li, and Zhang Junhua, 2001: GMS5 remote sensing of aerosol optical thickness over Chaohu Lake. *Acta Meteorologica Sinica Sinica*, **59**, 351–359.
- Mao Jietai, Liu Li, Zhang Junhua, Zhang Junhua, and Wang Meihu, 2002: summary comment on research of atmospheric aerosol in China. *Acta Meteorologica Sinica*, **60**, 625–634.
- Menon, S., J. Hansen, L. Nazarenko, and Y. Luo, 2002: Climate effects of black carbon aerosols in China and India. *Science*, **297**, 2250–2253.
- Molineaux, B., P. Ineichen, and N. O'Neill, 1998: Equivalence of pyrhelimetric and monochromatic aerosol optical depths at a single key wavelength. *Appl. Opt.*, **37**, 7008–7018.
- Qiu Jinhuan, 1998: A method to determine atmospheric aerosol optical depth using total direct solar radiation. *J. Atmos. Sci.*, **55**, 734–758.
- Qiu Jinhuan, 1999a: A method for spaceborne synthetic remote sensing of aerosol optical depth and vegetation reflectance. *Adv. Atmos. Sci.*, **15**, 17–30.
- Qiu Jinhuan, 1999b: Modified Delta-Eddington approximation for solar reflectance, transmission, and absorption calculation. *J. Atmos. Sci.*, **56**, 2955–2961.
- Qiu Jinhuan, 2001a: Broadband extinction method to determine atmospheric aerosol optical properties. *Tellus*, **53B**(1), 72–82.
- Qiu Jinhuan, 2001b: An improved model of surface BRDF-Atmospheric coupled radiation. *IEEE Trans. Geosci. Remote Sens.*, **39**, 181–187.
- Qiu Jinhuan, 2001c: A parameterized atmospheric correction model and its application simulation for satellite remote sensing. *Journal of Remote Sensing*, **5**, 401–406. (in Chinese)
- Qiu Jinhuan, 2002: A simple yet more accurate model to calculate solar radiative flux in the inhomogeneous atmosphere. *Adv. Atmos. Sci.*, **19**, 433–447.
- Qiu Jinhuan, 2003: Broadband extinction method to determine aerosol optical depth from accumulated solar direct radiation. *J. Appl. Meteor.*, **42**, 1611–1625.
- Qiu Jinhuan, and Yang Liquan, 2000: Variation characteristics of atmospheric aerosol optical depths and visibility in North China during 1980–1994. *Atmospheric Environment*, **34**, 603–609.
- Qiu Jinhuan, and Yang Liquan, 2002a: A study of retrieving aerosol optical depth from day- or hour-exposed broadband solar direct radiation. *Chinese J. Atmos. Sci.*, **26**, 449–458.
- Qiu Jinhuan, and Yang Liquan, 2002b: Broadband radiation methods to determine aerosol optical depth and imaginary part of its refractive index and their applications. *Proceedings of SPIE*, **4891**, 248–256.
- Qiu Jinhuan, Zheng Siping, Xia Qilin, Huan Qirong, Sun Jinhui, Wang Wenming, Pan Jidong, and Yang Liquan, 2002: A four-wavelength Lidar measurements of upper-tropospheric and stratospheric aerosol and ozone in Beijing. *Proc. 21th ILRC*, Quebec, Canada, 401–402.
- Qiu Jinhuan, Zheng Siping, Huang Qirong, Xia Qirong, Yang Liquan, Wang Wenming, Pan Jidong, and Sun Jinhui, 2003: Lidar measurements of cloud and aerosol in the upper troposphere in Beijing. *Chinese J. Atmos. Sci.*, **27**, 1–7.
- Penner, J. E., and coauthors, 1994: Quantifying and minimizing uncertainty of climate forcing by anthropogenic aerosols. *Bull. Amer. Meteor. Soc.*, **75**, 375–400.
- Stothers, R. B., 1996: Major optical depth perturbations to the stratosphere from volcanic eruptions: Pyrhelimetric period, 1881–1960. *J. Geophys. Res.*, **101**(D), 3901–3920.
- Yang Liquan, 1999: A study of wind measurements by Lidar based on the correction-analysis technique. Ph. D. dissertation, Instituta of Atmospheric Physics, Chinese Academy of Sciences.
- Yao, Z. Y., G. H. Wang, L. G. You, Y. H. Liu, W. B. Li, Y. J. Zhu, and B. L. Zhao, 2001: Microwave remote sensing of cloud liquid water in Shouxian area. *Quart. J. Appl. Meteor.*, **12** (Suppl.), 89–95. (in Chinese)
- Vermote, E. F., D. Tanre, J. L. Deuze, M. Herman, and J. J. Morcrette, 1997: Second simulation of the satellite signal in the solar spectrum, 6S: An overview. *IEEE Trans. Geosci. Remote Sens.*, **35**, 675–686.
- Wang Pucui, Lu Daren, and Li Zhanqing, 2001: A Parameterization method for retrieving surface UVB radiation from satellite. *Chinese J. Atmos. Sci.*, **25**, 1–13.
- Wang Xiaoya, Zhu Wenyao, Yan Haojian, and Cheng Zongyi, 1999: Preliminary results of precipitable water vapor monitored by ground-based GPS. *Chinese J. Atmos. Sci.*, **23**, 333–336.
- Wei Chong, Lei Hengchi, and Shen Zhilai, 2001: Microwave radiometric measurement in the rainy atmosphere. *Quarterly Journal of Applied Meteorology*, **12**, 65–72. (in Chinese)

- Wei Dongjiao, and Qiu Jinhuan, 1998: Wideband method to retrieve the imaginary part of complex refractive index of atmospheric aerosols. Part I: Theory. *Chinese J. Atmos. Sci.*, **22**, 677–685.
- Wei Dongjiao, and Qiu Jinhuan, 2000: Wideband method to retrieve the imaginary part of complex refractive index of atmospheric aerosols. Part II: Comparative measurement and application. *Chinese J. Atmos. Sci.*, **24**, 145–151.
- Weng, F. Z., N. C. Grody, R. R. Ferraro, A. Basist, and D. Forsyth, 1997: Cloud liquid water climatology from the Special Sensor Microwave/Imager. *J. Climate*, **10**, 1086–1098.
- Wu Yonghua, Hu Huanling, Hu Shunxing, Zhou Jun, and Zhang Min, 2002: Measurements of thermal profiles in the stratosphere and lower mesosphere with Rayleigh scattering Lidar. *Chinese J. Atmos. Sci.*, **26**, 23–29.
- Zhang Junhua, Si Zhaojun, Mao Jietai, and Wang Meihua, 2003: Remote sensing aerosol optical depths over China with GMS-5 satellite. *Chinese J. Atmos. Sci.*, **27**, 23–35.
- Zhang Junhua, Si Zhaojun, Mao Jietai, Wang Meihua, Liu Li, and Mao Jietai, 2000a: Remote sensing of aerosol optical properties with multi-wavelength sun-photometer in the Damxung region, Tibetan Plateau. *Chinese J. Atmos. Sci.*, **24**, 549–558.
- Zhang Junhua, Si Zhaojun, Mao Jietai, Wang Meihua, Wang Meihua, and Mao Jietai, 2000b: Error analysis and correction for multi-wavelength sun-photometer aerosol remote sensing. *Chinese J. Atmos. Sci.*, **24**, 855–859.
- Zhang Yinchao, Hu Huanlin, Yang Gaochao, Liu Xiaoqun, Sao Shishen, and Deng Ming, 2002: Mobile Lidar system developed for atmosphere remote sensing. *Proceedings of SPIE*, **4893**, 150–158.
- Zhang Yinchao, and couthors, 2001: Progress on a mobile Lidar for atmospheric pollution monitoring. *Optic-Electron Technique*, **14**, 1–6.
- Zhang, Y. H., S. W. Zhang, K. Xu, and J. S. Jiang, 2002: Microwave sensor development in recent two years in China. *Chinese J. Space Sci.*, **22**(Suppl.), 185–189.
- Zhao Zengliang, and Mao Jietai, 1999: Simultaneous retrieval of optical characteristics of atmospheric aerosol and surface albedo. *Chinese J. Atmos. Sci.*, **23**, 722–732.
- Zheng Wenggang, Li Hongjun, Yang Guotao, and Gong Shusheng, 1999: Lidar detection of the atmospheric density and temperature over Wuhan. *Chinese J. Atmos. Sci.*, **23**, 397–400.
- Zhou Xiuji, Li Weiliang, and Luo Yunfeng, 1998: Numerical simulation of the aerosol radiative forcing and regional climate effect over China. *Chinese J. Atmos. Sci.*, **22**, 418–427.
- Xia Xiangao, and Wang Mingxing, 2001: A new method for inferring total ozone and aerosol optical thickness from multispectral extinction measurements using eigenvalue analysis. *Geophys. Res. Lett.*, **28**, 1997–1998.
- Xia Xiangao, and Wang Mingxing, 2002: Analysis of dust aerosol properties in North of China based on remote sensing data. Ph.D dissertation, Institute of Atmospheric Physics, Chinese Academy of Sciences, 162pp. (in Chinese)